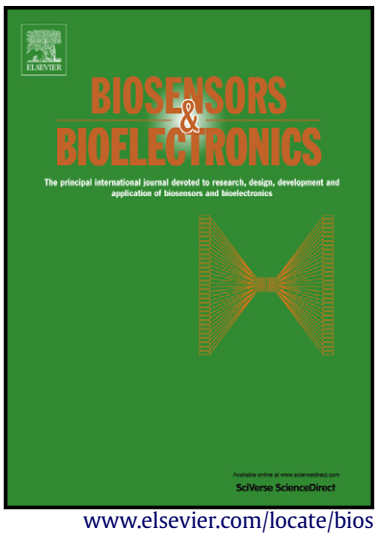

The transformation of common office supplies into a low-cost optical biosensing platform

Yong Duk Han, Hyeong Jin Chun, Hyun C. Yoon

www.elsevier.com/locate/bios

PII: S0956-5663(14)00218-8
DOI: http://dx.doi.org/10.1016/j.bios.2014.03.037
Reference: BIOS6665

To appear in: *Biosensors and Bioelectronics*

Received date: 19 December 2013
Revised date: 13 March 2014
Accepted date: 20 March 2014

Cite this article as: Yong Duk Han, Hyeong Jin Chun, Hyun C. Yoon, The transformation of common office supplies into a low-cost optical biosensing platform, *Biosensors and Bioelectronics,* http://dx.doi.org/10.1016/j.bios.2014.03.037

BIOS-D-13-02361, Revised Manuscript

The transformation of common office supplies into a low-cost optical biosensing platform

Yong Duk Han, Hyeong Jin Chun, and Hyun C. Yoon*

Department of Molecular Science & Technology, Ajou University, Suwon 443749, Korea

* Author to whom correspondence should be addressed.

E-mail: hcyoon@ajou.ac.kr

Tel: 82-31-219-2512

Fax: 82-31-219-2394

Abstract

By reassembling common office supplies, an optical biosensing system was developed. A laser pointer and the solar cell from a calculator were utilized in the developed optical biosensing system as the light source and signal transducer, respectively. For intuitive signal evaluation, a multimeter was used. The following two types of conventional enzymatic colorimetric assays were employed with the optical biosensing system: (i) the Trinder's reaction-based enzymatic assay; and (ii) the competitive enzyme-linked immunosorbent assay. These colorimetric assays were performed in reaction channels made from transparent polymer and glass. By matching the maximum absorption spectra of the colored end products from the assays with the emission spectra of the laser diodes, the biochemical reaction rate was manifested as a change in the intensity of the laser beam. This change was then converted by the solar cell into voltage and displayed on the connected multimeter. To verify the detection performance of the system, glucose and an osteoarthritis biomarker (urinary collagen type II C-telopeptide fragments [uCTX-II]) were quantified. With glucose, the voltages registered were linearly correlated with the glucose concentration, from 0 to 10 mM. Using a competitive immunoassay for uCTX-II, the system exhibited a calibration curve with a dynamic detection range between 1.3 and 10 ng/mL uCTX-II. Given the advantages of the proposed biosensing system, including its high sensitivity, facile fabrication, and the high obtainability and cost-effectiveness of the components used to make it, we expect that this study will provide a basis for the production of a low-cost optical biosensor.

Keywords: *Optical biosensor, Laser diode, Solar cell, Glucose monitoring, Osteoarthritis immunoassay*

1. Introduction

Since the first biosensor was reported by Clark and Lyons in 1962, advances in nanotechnology, material science, electronics, and optics have induced the innovation in analytical science and have offered the possibility of diagnosing disease using methods that are not restricted by constraints in time and space (Clark et al., 1962; Gubala et al., 2012; Turner, 2013). Among the various signal transducing technologies available in the biosensor field, the optical transducer is most widely used owing to its high accuracy and wide applicability (Borisov et al., 2008; Fan et al., 2008; Abbas et al., 2011). Based on this optical transducing technology, numerous optics-based analytical techniques have been developed, such as ultraviolet/visible (UV/Vis) spectroscopy, the fluorescence-based biochemical assay, and the surface plasmon resonance-based immunosensor (Homola, 2008; Laurent et al., 2008; Thomas et al., 2008; Sepúlveda et al., 2009; Newman et al., 2011). Regrettably, despite the progress in optical biosensing technologies, the use of commercialized optical biosensor products in point-of-care testing, which was the initial concept behind biosensor research, is rare (Yager et al., 2006; Whitesides, 2011). Although the use of state-of-the-art technologies and high-end optics systems in optical biosensors enables specific and accurate analysis, it inevitably brings drawbacks in terms of commercialization and portability, such as the excessive cost of optical components, the requirement for large amounts of electricity, the complicated arrangement of the optic components (e.g., lenses, mirrors, filters, prisms, photodiodes, and light sources), and the need to have a signal analyzer such as a computer in addition to the system itself. To overcome this limitation and to produce a user-friendly biosensor that minimizes the trade-off between analytical performance and device complexity, a more intuitive, cost-effective and easy-to-use optical signal transducing system is required. Thus, we have focused on the simplification of the conventional optical transducing system, which is still based on the analytical principles of UV/Vis spectroscopy, but employs common electronic components that can be found in everyday life.

Briefly, a UV/Vis spectrophotometer is composed of a light source that is capable of providing a wide spectrum of wavelengths and a photodetector (Thomas et al., 2008). When light of a particular wavelength is passed through a sample, if the wavelength corresponds to the absorption spectrum of the analyte in the sample, the sample will absorb the light and thus reduce its intensity. By analyzing the change in light intensity, it is then possible to quantify the analyte in the sample. Although spectrophotometers enable simple and intuitive analysis of samples, the configuration of the optics systems and other components in spectrophotometers is complicated.

Recently, rapid growth in the field of optical data storage (e.g., compact discs and digital video discs) has led to a reduction in the price of the optoelectronic components such as laser diodes and photovoltaic cells (solar cells) and, consequently, their use in laser pointers and solar-powered digital calculators, respectively, has increased. Unlike the light source used in UV/Vis spectroscopy, the laser diode in a laser pointer provides well-defined, single spectrum light, with low power consumption (3 - 5 V). The solar cell in a digital calculator simply generates a direct circuit (DC) voltage when the calculator is exposed to light. Due to the impressive optical properties and cost-effectiveness of the laser diode and the solar cell, we focused on these common electronic components as substitutes for the optical components normally found in conventional optics systems to develop a new optical biosensing system.

In this study, we constructed a simple optical biosensing system, based on the principles of UV/Vis spectroscopy, by assembling common electronic components, as shown in Figure 1. The laser diode from a laser pointer, the solar cell from a digital calculator, and a digital multimeter were utilized as the light source, optical receiver, and signal analyzer, respectively, for an optical transducing system. In this system, when the laser diode light reaches the solar cell, light intensity is converted into DC voltage, which can then be measured using the multimeter. Colorimetric biorecognition reactions can then be carried out in a disposable biosensing channel located between the laser diode and the solar cell. As depicted in Figure 2A, biochemical reaction-mediated changes in light intensity are simply indicated on the multimeter as changes in voltage. By tracing these voltage changes, it is possible to use the optical transducing system like a conventional spectrophotometer to quantify the concentration of an analyte. To validate the analytical performance of this system, a glucose oxidase (GOx)/horseradish peroxidase (HRP)-mediated glucose assay based on Trinder's reaction (Figure 2B) (Tamaoku et al., 1982; Nakamura et al., 2008) and a competitive enzyme-linked immunosorbent assay (ELISA) for the detection of an osteoarthritis (OA) biomarker (urinary collagen type II C-telopeptide fragments [uCTX-II]) (Reijman et al., 2004; Garnero et al., 2005) using 3,3′,5,5′-tetramethylbenzidine (TMB) as the chromogenic substrate (Figure 2C) (Tatzber et al., 2003; Szili et al., 2011) were conducted; both of these assays generate a blue-colored reaction product. As the laser diode modules (635 and 655 nm) emit light matching the absorption spectra of the end products from the glucose and uCTX-II assays (λ_{max} = 630 nm and 652 nm, respectively), it was possible to measure the concentrations of the enzymatic end products via the principles of UV/Vis spectroscopy. To construct target-specific biorecognition layers for each biochemical assay on the biosensing channel, which was composed of glass and polydimethylsiloxane (PDMS), a polydopamine-mediated surface

modification strategy was used (Lee et al., 2007). Using the optical transducing system and target-specific biosensing channel, we were able to efficiently quantify the concentrations of glucose (1.25-20 mM) and uCTX-II (1.3-10 ng/mL). Furthermore, the sensitivity of the biosensing system could be adjusted by controlling the numbers of enzyme layers, as demonstrated with the glucose assay. Thus, in this paper, we present an experimental demonstration of the concept of an optical biosensing system made with common electronic components, as well as an assessment of its analytical performance.

2. Experimental

2.1 Material and apparatus

Dopamine hydrochloride and GOx (from *Aspergillus niger*) were purchased from Sigma. 4-Aminoantipyrine (4-AAP) and Tris(hydroxymethyl)aminomethane (Tris) were obtained from Sigma-Aldrich. Amine-terminated G4 polyamidoamine (PAMAM) dendrimer was purchased from Aldrich. 3,3′-Dithiobis[sulfosuccinimidylpropionate] (DTSSP) and the TMB substrate solution were obtained from Pierce. HRP was purchased from Toyobo enzyme. N-Ethyl-N-(2-hydroxy-3-sulfopropyl)-3,5-dimethylaniline (MAOS) was obtained from Dojindo. The peptide fragments EKGPDP and PEG_4-EKGPDP were synthesized and provided by Peptron Inc. An uCTX-II ELISA kit including an HRP-labelled monoclonal anti-uCTX-II antibody was obtained from Immunodiagnostic Systems. Sylgard® 184 silicone elastomer kit was purchased from Dow Corning. For solutions, doubly distilled and deionized water (dH_2O) was used. Laser diode modules (635 and 655 nm) were obtained from AixiZ. The miniature solar cell (BPW34) was purchased from Vishay. A multimeter was obtained from Sanwa Electric Instrument.

2.2 Construction of the optical transducer using common office supplies

A signal transducer including a light source, light-receiving element, and signal reader was designed and constructed using a commercial laser diode that can be found in a laser pointer, a miniature solar cell that is used in a digital calculator, and a multimeter, respectively. As shown in Figure 1A, to provide a dark environment for the optical biosensing, the plastic casing from a compact disc player was used. The miniature solar cell with two legs (positive and negative) was assembled on a PCB board, and each leg was soldered with copper wires. The resulting mini solar cell was fastened at the bottom of the casing with double-sided adhesive tape. The free ends

of the soldered wires were taken out of the casing and connected to the multimeter. The sensitive area of the solar cell was 0.75 cm^2. An 8-mm hole was drilled in the cover of the plastic casing at a point with the same x- and y-positions as those of the solar cell on the bottom of the casing. As depicted in Figure 1B, the laser diode was fastened in the drilled spot on the cover with double-sided adhesive tape. The laser diode module was then connected to the battery-based power supplier (3.7 V) containing an on/off switch. When the switch is turned on, laser light shines on the solar cell on the bottom of the casing. The voltage generated from the solar cell was displayed on the connected multimeter. The solar cell generated approximately 300 mV and 560 mV for the 635 nm laser diode and the 655 nm laser diode, respectively.

2. 3 Fabrication and surface modification of the reaction channel

The biosensing channel is made of PDMS at the top and slide glass at the bottom. The molds for casting the PDMS tops were made of aluminum. Computer numerical control machining was used to fabricate the specific structures including channels and holes (Figure S1A of the Supplementary Information). A 10:1 (v/v) mixture of PDMS monomer and its curing agent was poured onto the aluminum mold and cured at 150 °C for 20 min in a vacuum oven (Ko et al., 2003). Then, the solidified PDMS substrate was peeled off from the aluminum mold and rinsed with dH_2O. The rinsed substrates were dried in a vacuum oven at 150 °C for 15 min. Each fabricated PDMS top contained three channels (3 mm in width × 18 mm in length × 1.5 mm in depth). Individual channels have inlet and outlet holes. The slide glass bottom substrates were washed with ethanol and dH_2O. Using the corona plasma treatment method, the PDMS top and glass bottom was attached as shown in Figure S1B of the Supplementary Information (Kim et al., 2010). The resulting PDMS-glass substrates were incubated at 150 °C for 10 min. The volume of each channel was 90 μL.

For construction of the biorecognition layer on the inside surface of the channel, a polydopamine coating strategy was employed (Lee et al., 2007). Briefly, 2 mg/mL of dopamine hydrochloride was dissolved in 10 mM Tris-HCl buffer solution, and the pH of the solution was adjusted to 8.5. The pH-adjusted dopamine solution was immediately injected into the prepared reaction channels and allowed to incubate for 24 h at room temperature in a darkroom. After then, each channel was rinsed with dH_2O. The resulting polydopamine-coated reaction channels were filled with dH_2O and stored at 4 °C until further biomolecular modification. Although the resulting channels had a slight brown color, the inherent transparency of the PDMS and glass substrates was maintained, as is shown in Figure S1C of the Supplementary Information. Because the intensity of the

absorption spectra of surface-bound polydopamine is very weak, we anticipated that the subsequent experiments would not be affected by the color of the polydopamine layer (Figure S1D of the Supplementary Information).

2.4 Fabrication of the biorecognition layer for glucose biosensing and competitive immunosensing

To fabricate the multi-enzyme layer for the glucose assay, a layer-by-layer technique employing dendrimer was utilized, as depicted in Figure 3A (Yoon and Kim, 2000). First, an aqueous G4 PAMAM dendrimer (0.5%) solution was prepared by dissolving the dendrimer stocks in 0.1 M phosphate-buffered saline solution (PBS, pH 8.0). The dendrimer solution was then injected into the polydopamine-coated channels and incubated for 16 h at room temperature. Next, the channels were washed with PBS (pH 8.0) and then filled with 20 mM ethanolamine to block any unreacted functional moieties in the polydopamine layer. After 15 min, the channels were rinsed again with PBS (pH 8.0). Prior to adding the enzyme layers, a simple glycan-oxidization step was performed on HRP and GOx using 40 μM sodium periodate to convert the carbohydrate moiety on each enzyme to an aldehyde group. For the HRP layer, 1 mg/mL of oxidized HRP solution (PBS, pH 6.8) was applied to a dendrimer-coated reaction channel for 1 h. Next, an intermediate dendrimer layer was constructed above the HRP layer by injecting aqueous G4 PAMAM dendrimer solution into the channel and incubating for 1 h, followed by rinsing. After the channel was washed with PBS (pH 7.2), 1 mg/mL of oxidized GOx solution (PBS, pH 6.8) was then loaded into the channel and allowed to incubate for 1 h. The resulting multilayer structure (dendrimer/HRP/dendrimer/GOx) was considered a single multi-enzyme layer (MEL1) unit. By repeating the enzyme-layer forming procedures described above, double and triple multi-enzyme layer (MEL2 and MEL3, respectively) units were constructed.

To construct the bioreceptor layer for the competitive uCTX-II immunoassay, peptide immobilization via self-assembly of monolayer was used, as shown in Figure 3B. First, 5 mM DTSSP solution (PBS, pH 8.0) was loaded into the polydopamine-coated reaction channel and incubated for 3 h at room temperature. After washing, 20 μg/mL of amine-terminated PEG_4-EKGPDP peptide was applied to the channel for 1 h. The synthesized peptide was covalently immobilized on the channel surface via amide bond formation between the amine groups of the peptide and the N-hydroxysulfosuccinimide moiety of DTSSP. To block any unreacted amine-reactive moieties of polydopamine and DTSSP on the channel surface, 20 mM ethanolamine was injected in to the channel and allowed to react for 15 min. All the enzyme-modified and peptide-immobilized reaction channels were filled with PBS (pH 7.2) and stored at 4 °C until the biochemical assay. X-ray photoelectron spectrometry

(XPS) analysis was used to characterize the chemically functionalized biosensing channel surface. Detailed descriptions and additional information for XPS are provided in Figure S2 in the Supplementary Information.

2.5 Validation of the optical biosensing principle

To verify the optical biosensing principle, changes in laser light spectra in response to the progress of biochemical reactions were observed and analyzed using a modular spectrometer. Prior to the biochemical assay, the laser source was aligned with the light-receiving part of the spectrometer. For validation of the optical glucose biosensing system, four samples with different concentrations of glucose (0, 1.25, 5, and 20 mM) were prepared in PBS (pH 7.2) and then mixed with Trinder's reagent solution containing 20 mM 4-AAP and 2 mM MAOS at a 1:1 ratio. The resulting solutions were then each injected into a different MEL1 channel and allowed to react for 10 min. After the enzymatic reaction, the test channels in which the solutions had turned blue were placed between the laser light and the spectrometer. Under darkroom condition, the 635-nm laser diode was turned on, and changes in emission spectra of incident light were measured with the spectrometer.

To validate the optical biosensing system using an immunoassay, four reaction channels that were modified with four different PEG_4-EKGPDP concentrations (0, 0.4, 4, and 40 μg/mL) were prepared. Next, HRP-labelled anti-CTX-II antibody solution was injected into the channels and allowed to react for 10 min. After washing, a TMB substrate solution containing H_2O_2 was applied and allowed to react for 5 min. Then, alterations in emission spectra of light from the 655 nm laser diode were measured for each channel.

2.6 Detection of glucose and uCTX-II using the optical biosensing system

To demonstrate the analytical performance of the designed biosensing system, calibration studies for glucose and uCTX-II were performed using the developed optical transducer and bioreceptor-modified reaction channel. For glucose calibration, glucose samples in various concentrations (0, 1.25, 2.5, 5, 10 and 20 mM in PBS, pH 7.2) were mixed with Trinder's reagent solution as described above and then allowed to react. Prior to the assay, the multi-enzyme-modified reaction channels (MEL1, MEL2, and MEL3) were installed in the transducer and the laser light (635 nm) and multimeter were turned on. Immediately after loading the solutions into the reaction channels, the cage cover was closed. The displayed DC voltage on the multimeter was recorded on a minute-by-minute basis during the 10 min of reaction time. The calibration results from the three types of reaction channels (MEL1, MEL2, and MEL3) were compared.

For the uCTX-II assay, uCTX-II samples in various concentrations (0, 1.3, 2.5, 5, and 10 ng/mL) and reaction channels that had been modified using 20 μg/mL of PEG_4-EKGPDP were utilized. The samples were mixed with the HRP-conjugated anti-CTX-II antibody from the uCTX-II ELISA kit in a 1:3 volumetric ratio for 1 h. The mixtures were then loaded into the peptide-modified reaction channels and incubated for 30 min. After rinsing, TMB reagent was injected into the resulting channels, which were then installed into the optical transducing system. Using 655-nm laser, changes in voltage during the 5 min of reaction time were recorded on a minute-by-minute basis. To assess the reproducibility of the developed biosensing system, the inter-assay coefficients of variation (COV) were calculated by measuring the same samples (glucose and uCTX-II) using five independent sensing channels.

3. Results and discussion

3.1 Signaling principle of the optical biosensing system

Our biosensing system used an optical transducer in combination with an HRP-mediated, colorimetric biochemical assay. As is widely known, the enzymatic reaction between HRP and H_2O_2 induces the conversion of certain colorless chromogenic substrates into colored products with specific absorption spectra. The amount of these colored products and the extent of absorbance at specific wavelengths is changed in proportion to the analyte concentration (Figure 2A). In this study, of the various chromogenic substrates available, Trinder's reagent (4-AAP and MAOS) and TMB were used for glucose detection and uCTX-II detection, respectively.

In the case of the glucose assay, in the presence of glucose and Trinder's reagent, the multi-enzyme reaction of GOx and HRP generated a blue-colored product that exhibited a maximum absorption wavelength (630 nm) that overlapped with the emission spectra from the 635-nm laser light, as shown in Figure 2B. During the glucose detection procedure, the blue-colored products which were produced by the glucose assay in the reaction channel absorbed the emitted laser light, thereby reducing the intensity of the light arriving to the solar cell. Consequently, the reduction in light intensity is inversely proportional to the concentration of glucose, and we could recognize the changes in light intensity as voltage changes using the multimeter.

Our biosensing system is also able to utilize the conventional TMB substrate, which is widely used in ELISAs as a chromogenic substrate. In the presence of H_2O_2, TMB is oxidized by HRP and converted into a blue-colored product with maximum absorption at 370 nm and 652 nm, as shown in Figure 2C. In general, the extent

of increase in maximum absorption is proportional to the amount of HRP. In this study, it was possible to detect uCTX-II using a competitive ELISA because uCTX-II contains a monomeric EKGPDP epitope. As an antigen analogue of uCTX-II, PEG-conjugated EKGPDP peptides (20 μg/mL) were immobilized on the channel surface via DTSSP-assisted amide bond formation. To the analogue-prepared surface, a solution containing a mixture of free EKGPDP and HRP-conjugated anti-CTX-II antibody was applied, followed by the TMB reaction. In the uCTX-II competitive ELISA, the amount of surface-bound HRP-conjugated anti-CTX-II antibodies is inversely proportional to the analyte (uCTX-II) concentration. As the absorption wavelength of the oxidized TMB (652 nm) overlaps with that of the applied laser light (655 nm), the laser light is absorbed and the intensity of light is reduced when it passes through the resulting reaction channel. In contrast to the glucose detection assay, the displayed voltage is proportionally decreased with the decrease in uCTX-II concentration, based on the features of competitive ELISA.

3.2 Verification of the developed optical transducing principle

In the optical biosensing system, the final intensity of the laser light is dependent on the concentration of the analyte as determined by the biochemical reaction in the biosensing channel, and these alterations in laser intensity are transduced into changes in voltage by the solar cell. To clearly show the correlation between laser intensity changes and the biochemical reaction ratio related to analyte concentration, we also measured spectral changes in laser light passed through the biosensing channel as a function of the change in analyte concentrations using a modular spectrometer.

To assess the correlation between changes in intensity of light from a 635-nm laser and the changes in glucose concentration using the Trinder's reaction-based glucose assay, four different concentrations (0, 1.25, 5, and 20 mM) of glucose samples were examined. As shown in Figure 4A, the height of the 635-nm laser spectrum decreased in accordance with the increase in glucose concentration. These results suggest that the light from the 635-nm laser diodes was sufficiently absorbed by the enzymatic product from the Trinder's reaction-based glucose assay because the reactant absorption spectrum and the emission spectrum of the 635-nm laser are well matched, as shown in Figure 4B.

By using a 655-nm laser, the HRP-TMB reaction-based optical signaling principle was verified. To the prepared biosensing channels that had been modified with antigen analogues in various concentrations (0, 1.3, 5, and 20 μg/mL of PEG_4-EKGPDP), HRP-conjugated anti-CTX-II antibody was applied, followed by the TMB

reaction. In this case, the concentration of HRP-tagged antibody is proportional to the concentration of PEG_4-EKGPDP. Consequently, the concentration of enzymatic product (the oxidized TMB) is also proportional to the quantities of antigen analogues. As shown in Figure 4C, the intensity of laser light readily decreased according to the increase in concentration of antigen analogues. The results of the 635-nm laser tests indicated that the laser light was properly absorbed by the enzymatic product due to overlapping of the laser emission spectra (655 nm) with the absorption spectra of the oxidized TMB, as depicted in Figure 4D. Based on these observations, we conclude that this transducing platform can be used for optical biosensing.

3.3 Glucose detection and sensitivity control

As a model study for application of the optical biosensing system, glucose quantification was performed. Initially, glucose samples in a concentration range of 0 to 20 mM were measured using MEL1 biosensing channels. As shown in Figure 5A, during the 10 min reaction time, the color intensity of the solutions in the channels increased in proportion with the concentration of glucose. In the presence of glucose, the DC voltages from each biosensing channel decreased linearly during the reaction time. Contrastingly, DC voltages from a blank sample containing no glucose did not change. The extent of the reduction in voltage increased in proportion to the increase in glucose concentration, as expected. To demonstrate the correlation between changes in absorbance of enzymatic reactant and alterations in DC voltage, absorption spectra of individual reactants in biosensing channels were analyzed by UV/Vis spectroscopy and compared with the registered DC voltage signals. As shown in Figure S3A of the Supplementary Information, absorbance at 630 nm of enzymatic reactants increased in proportion to the glucose concentration. Interestingly, the trend in DC voltage alteration was symmetrical to the absorbance changes. The same correlation was observed in subsequent test results using MEL2 and MEL3 (Figure S3B and S3C of the Supplementary Information). These results indicate that the principle of UV/Vis spectroscopy was properly embodied in the optical biosensing system and that glucose could be detected using this system.

We next tried to improve the sensitivity of the system by increasing the number of enzyme (GOx-HRP) layers, as we anticipated that the signal response would be regulated by the number of signaling enzyme layers (Yoon and Kim, 2000; Han et al., 2011). As shown in Figure 5B, the intensity of the color in MEL2 channels containing two bi-enzyme (GOx-HRP) layers was greater than that in the MEL1 test. In addition, DC voltage signals from MEL2 channels were more steeply decreased compared to those from MEL1 channels. Likewise,

the signal response of the MEL3 channel, which contained three bi-enzyme layers, was more sensitive than that of the MEL2 channel (Figure 5C). Based on the glucose detection results from the MEL1, MEL2, and MEL3 channels (right graphs of Figure 5A, 5B, and 5C), their calibration curves were plotted in Figure 5D. The changes in DC voltages (ΔDC voltage) were calculated using the following formula:

$$\Delta\text{DC voltage} = (\text{DC voltage at 0 min}) - (\text{DC voltage at 10 min}) \quad (1)$$

In all of the calibration curves, ΔDC voltage signals linearly increased in the range of 0 to 10 mM of glucose concentration and saturated at concentrations above 10 mM of glucose. The slopes of the linear dynamic range (0-10 mM) on the calibration curve from MEL1, MEL2, and MEL3 were 2.8 mV/mM, 3.6 mV/mM, and 4.7 mV/mM, respectively. These results indicate that the signal response ratio of the biosensor to the glucose concentration was improved by approximately 30% with each addition of bi-enzyme layers on the biosensing channel surface. These trends were also observed in the limit of detection (LOD) values. The LOD values of the proposed glucose biosensing channels, MEL1, MEL2, and MEL3, calculated as three times the standard deviation of the background signal, were 0.82 mM, 0.63 mM, and 0.43 mM, respectively. These results demonstrate that the sensitivity of the optical biosensing system for glucose detection can be easily regulated by controlling the number of enzyme layers. Considering that the minimum detection level of a commercial glucose meter is 0.5 mM, the acquired LOD value from MEL3-based glucose biosensing (0.43 mM) may be evidence of the potential applicability of our biosensing system for practical glucose monitoring. The inter-assay coefficient of variation (COV) of the MEL3-based glucose biosensor was 8.3%.

3.4 Competitive immunosensing of uCTX-II

To assess the applicability of the optical biosensing system for immunoassays, quantitative immunoanalysis for a disease biomarker was performed. As a model biomarker, uCTX-II, which is one of the principal biomarkers for OA diagnosis, was chosen (Reijman et al., 2004; Garnero et al., 2005). During OA progression, cartilage matrix such as collagen is degraded by collagenase and released from the damaged cartilage tissue (Elsaid and Chichester, 2006). The C-telopeptide fragments of type II collagen (CTX-II) is one of the collagen degradation products. The CTX-II molecules are released from the synovial fluid in the cartilage into bodily fluids, such as serum, and are ultimately excreted through the urine as urinary CTX-II (uCTX-II). In contrast to

the serum CTX-II, which contains a cross-linked dimeric epitope (EKGPDP), uCTX-II contains the monomeric EKGPDP epitope or a variant monomeric epitope (Birmingham et al., 2006; Eyre et al., 2008). Based on this structural property of uCTX-II, a competitive assay for uCTX-II detection was recently developed and commercialized as an ELISA kit. In the present study, we incorporated the principle underlying the competitive immunoassay for uCTX-II detection in the developed optical biosensing system. To prepare the competitive immunosensing surface, 20 μg/mL of PEG_4-EKGPDP was immobilized in the biosensing channel. Various concentrations (0-10 ng/mL) of uCTX-II were pre-mixed with HRP-conjugated anti-CTX-II antibody from the uCTX-II ELISA kit and applied to the prepared uCTX-II biosensing channel. Based on the competition immunoassay principle, only the HRP-conjugated antibodies that had not interacted with the free uCTX-II could bind with the PEG_4-EKGPDP on the surface of the biosensing channel. Consequently, the quantities of surface-bound HRP-labelled antibodies are in inverse proportion to the concentration of the free antigen. Based on this principle, the color intensity of the HRP-TMB reaction product decreased according to the increase in target antigen (Figure 6A). Accordingly, the height of the absorption spectra also decreased in proportion to the antigen concentration, as shown in Figure S4A of the Supplementary Information. In our biosensing system, this decrease in absorbance causes the DC voltage to increase accordingly. As depicted in Figure 6B, DC voltage increased according to the decrease in antigen concentration. The inverse correlation between absorbance and DC voltage alteration is shown in Figure S4B of the Supplementary Information and indicates that the competitive uCTX-II immunoassay worked properly in this system. Using the immunoassay results, a calibration curve was plotted in Figure 6C using equation (1). The DC voltage exponentially decreased according to EKGPDP concentration from 1.3 to 10 ng/mL. The LOD value, calculated as three times the standard deviation of the blank signal, was as low as 0.3 ng/mL. The calculated inter-assay COV of the uCTX-II detection was 7.2%. The acquired detection range and LOD from the uCTX-II immunoassays cover the clinically required level for OA diagnosis (1-10 ng/mL uCTX-II). On the basis of these results, we conclude that our system could be applied to practical immunoanalysis.

4. Conclusions

Without using complicated and expensive technical equipment, an optical biosensing system was developed by assembling common electronic components that can be found as standard office supplies. Using this system,

sensitive detection of glucose and an OA biomarker was possible even though no specialized tools were involved. Additionally, this system provides numerous advantages such as low-cost manufacturing, facile fabrication, and intuitive signal transducing. In addition, all the biosensing procedures, including light generation, signal transducing, signal evaluation, and display, can be operated with common batteries. The most important feature of the developed biosensing platform is its high applicability in numerous fields of study. Our biosensing system allows the use of all assays that utilize HRP. As needed, the biorecognition layer in the biosensing channel can be changed. Based on these features and merits, we hope that our biosensing system will be a useful platform under conditions of limited resources. The validation of this biosensing strategy for the diagnostic application using bodily fluid samples will be achieved through collaboration with clinicians, which is currently underway.

Acknowledgement

This research was supported by the Korean Ministry for Health, Welfare, and Family Affairs (A091120) and the Priority Research Centers Program (2009-0093826).

References

Abbas, A., Linman, M. J., Cheng, Q., 2011. Biosens. Bioelectron. 26, 1815-1824.

Birmingham, J. D., Vilim, V., Kraus, V. B., 2006. Biomarker Insights 1, 61-76.

Borisov, S. M., Wolfbeis, O. S., 2008. Chem. Rev. 108, 423-461.

Clark, L. Jr., Lyons, C., 1962. Ann. NY. Acad. Sci. 102, 29-45.

Elsaid, K. A., Chichester, C. O., 20006. Clin. Chim. Acta 365, 68-77.

Eyre, D. R., Weis, M. A., Wu, J. -J., 2008. Methods 45, 65-74.

Fan, X., M. I., White, Shopova, S. I., Zhu, H., Suter, J. D., Sun, Y., 2008. Anal. Chim. Acta 620, 8-26.

Garnero, P., Peterfy, C., Zaim, S., Schoenharting, M., 2005. Arthritis Rheum. 52, 2822–2829.

Gubala, V., Harris, L. F., Ricco, A. J., Tan, M. X., Williams, D. E., 2012. Anal. Chem. 84, 487-515.

Han, Y. D., Song, S. Y., Lee, J. H., Lee, D. S., Yoon, H. C., 2011. Anal. Bioanal. Chem. 400, 797-805.

Homola, J., 2008. Chem. Rev. 108, 462-493.

Kim, K., Park, S. W., Yang, S., 2010. BioChip J. 4, 148-154.

Ko, J. S., Yoon, H. C., Yang, H., Pyo, H. -B., Chung, K. H., Kim, S. J., Kim, Y. T., 2003. Lab Chip 3, 106-113.

Laurent, N., Voglmeir, J., Flitsch, S. L., 2008. Chem. Commun. 37, 4400-4412.

Lee, H., Dellatore, S. M., Miller, W. M., Messersmith, P. B., 2007. Science 318, 426-430.

Nakamura, H., Mogi, Y., Akimoto, T., Naemura, K., Kato, T., Yano, K., Karube, I., 2008. Biosens. Bioelectron. 24, 455-460.

Newman, R. H., Fosbrink, M. D., Zhang, J., 2011. Chem. Rev. 111, 3614-3666.

Reijman, M., Hazes, J. M., Bierma-Zeinstra, S. M., Koes, B. W., Christgau, S., Christiansen, C., Uitterlinden, A. G., Pols, H. A., 2004. Arthritis Rheum. 50, 2471–2478.

Sepúlveda, B., Angelomé, P. C., Lechuga, L. M., Liz-Marzán, L. M., 2009. Nano Today 4, 244-251.

Szili, E. J., Jane, A., Low, S. P., Sweetman, M., Macardle, P., Kumard, S., St. C. Smarte, R., Voelcker, N. H., 2011. Sens. Actuat. B:Chem. 160, 341-348.

Tamaoku, K., Murao, Y., Akiura, K., 1982. Anal. Chim. Acta 136, 121-127.

Tatzber, F., Griebenow, S., Wonisch, W., Winkler, R., 2003. Anal. Biochem. 316, 147-153.

Thomas, M. J. K., Ando, D. J., 2008. Ultraviolet and visible spectroscopy: analytical chemistry by open learning. 2nd edition, Wiley India Pvt. Limited.

Turner, A. P. F., 2013, Chem. Soc. Rev. 42, 3184-3196.

Whitesides, G. M., 2011. Lab Chip 11, 191-193.

Yager, P., Edwards, T., Fu, E., Helton, K., Nelson, K., Tam, M. R., Weigl, B. H., 2006. Nature 442, 412-418.

Yoon, H. C., Kim, H. -S., 2000. Anal. Chem. 72, 922-926.

Figure Caption

Figure 1. Configuration of the optical biosensor system. (A) Outside appearance of the developed biosensor. (B) Inside structure of the optical biosensor system.

Figure 2. Schematic illustration of the principles used to develop the optical biosensor system. (C) The optical transducer. The intensity of the laser light on the solar cell decreases according to the increase in absorbance in the biosensing channel. The change in light intensity is displayed as a DC voltage signal on the multimeter. (B) Trinder's reagent-based glucose detection. GOx and HRP are used in the bi-enzymatic colorimetric glucose assay. (C) Reaction scheme of HRP-mediated color development using the chromogenic substrate TMB.

Figure 3. Workflow of the construction of the bioreceptor layer in the biosensing channel. (A) Fabrication of the bi-enzyme layers used for glucose biosensing using GOx, HRP, and a dendrimer. (B) Construction of the immunosensing layer using the antigen analog PEG_4-EKGPDP for uCTX-II detection.

Figure 4. (A) Changes in the emission spectra of a 635-nm laser light caused by different concentrations of glucose (0, 1.25, 5, and 20 mM). (B) Absorption spectrum of the enzymatic end-product from the glucose assay (closed black square) and emission spectrum of the 635-nm laser light. (C) Changes in the emission spectra of a 655-nm laser light caused by different concentrations of surface-bound PEG_4-EKGPDP (0, 1.3, 5, and 20 μg/mL). (D) Absorption spectrum of the end-product obtained from the HRP-TMB reaction (closed red triangle) and emission spectrum of the 655-nm laser light. The absorption spectra of enzymatic end-product and the emission spectra of laser light were observed by using a UV/Vis spectrophotometer and a modular spectrometer, respectively.

Figure 5. Glucose biosensing results. Various concentrations of glucose (0, 1.25, 2.5, 5, 10, and 20 mM) were measured using the optical biosensing system. (A) Image of the glucose assay MEL1 biosensing channels (left) and a graph showing the DC voltage decrease in response to increasing concentrations of glucose (right). (B) Image of the glucose assay MEL2 biosensing channels (left) and a graph showing the DC voltage decrease in response to increasing concentrations of glucose (right). (C) Image of the glucose assay MEL3 biosensing

channels (left) and DC voltage decay in response to increasing concentrations of glucose (right). (D) Calibration results for the MEL1 biosensing channel (closed black square), the MEL2 channel (closed red circle), and the MEL3 channel (closed blue triangle). The dashed lines indicate the dynamic linear ranges (from 1.25 mM to 10 mM glucose) of the individual biosensing channels.

Figure 6. Results of uCTX-II detection. Free uCTX-II samples in various concentrations (0, 1.3, 2.5, 5, and 10 ng/mL) were measured using the optical biosensing system. (A) Image of the channels used for the uCTX-II immunoassay. (B) Changes in DC voltages according to uCTX-II concentration. (C) Calibration curve for uCTX-II.

Figure 1

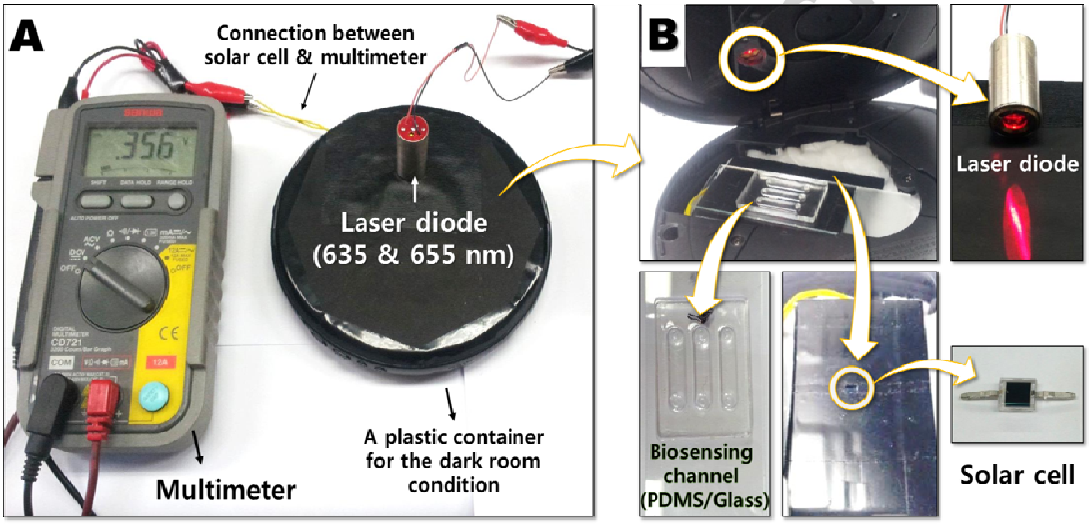
A
Connection between
solar cell & multimeter
Laser diode
(635 & 655 nm)
A plastic container
for the dark room
condition
Multimeter
B
Laser diode
Biosensing
channel
(PDMS/Glass)
Solar cell

Figure 2

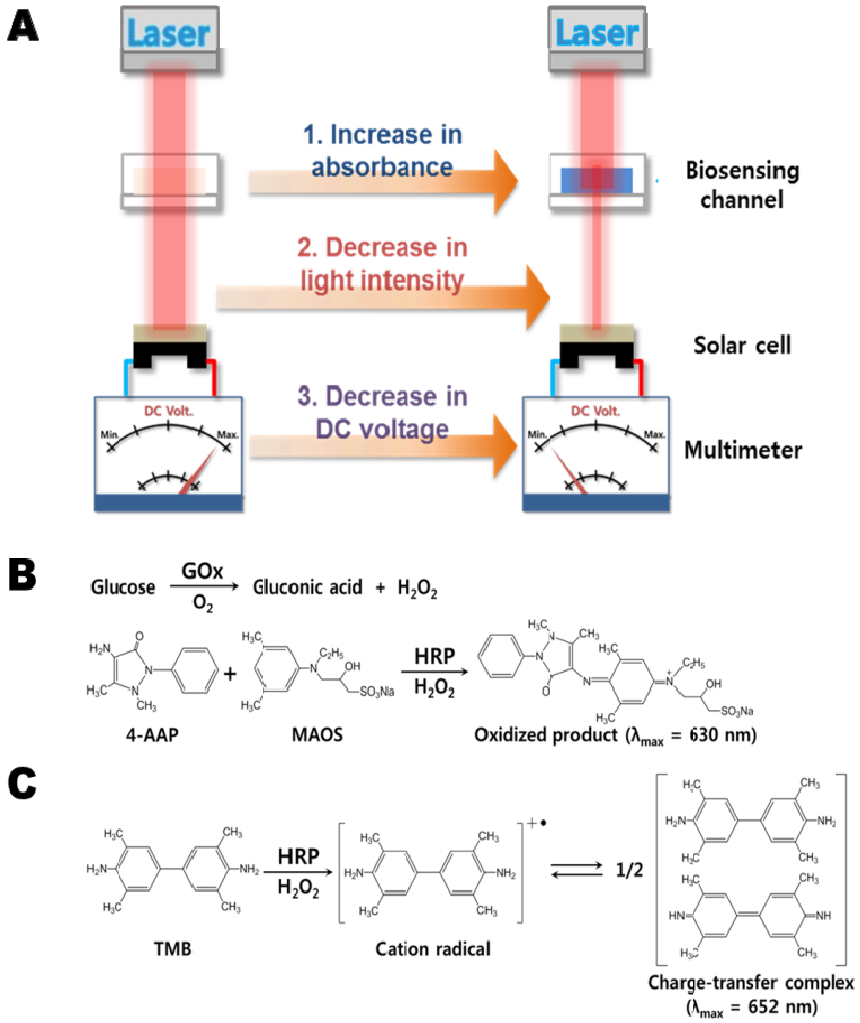
A
Laser
Laser
1. Increase in absorbance
Biosensing channel
2. Decrease in light intensity
Solar cell
3. Decrease in DC voltage
Multimeter
DC Volt.
Min.
Max.
B
Glucose
GOx
O2
Gluconic acid + H2O2
HRP
H2O2
4-AAP
MAOS
Oxidized product (λmax = 630 nm)
C
HRP
H2O2
1/2
TMB
Cation radical
Charge-transfer complex
(λmax = 652 nm)

Figure 3

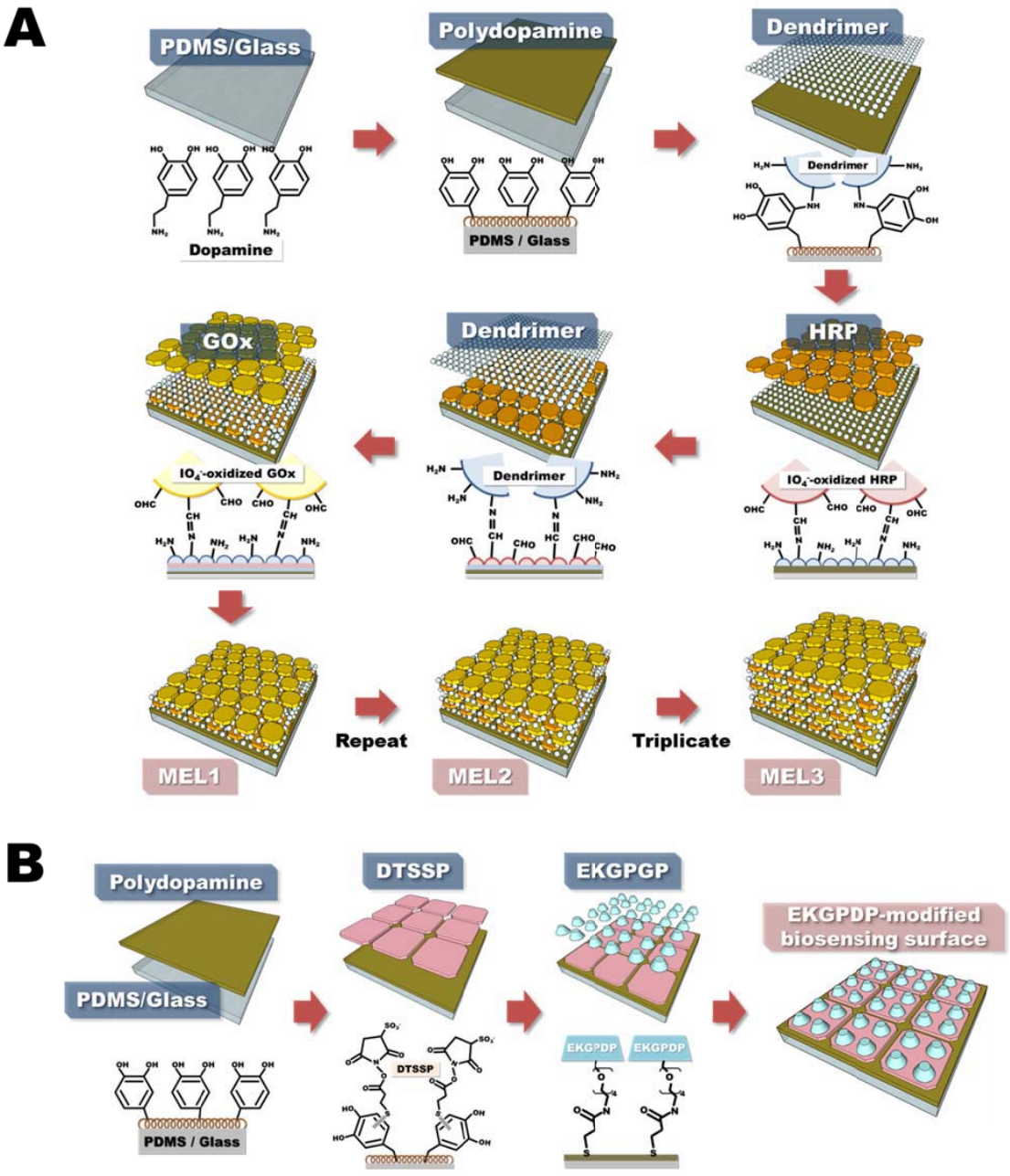
A
PDMS/Glass
Dopamine
Polydopamine
PDMS / Glass
Dendrimer
Dendrimer
HRP
IO4-oxidized HRP
Dendrimer
Dendrimer
GOx
IO4-oxidized GOx
MEL1
Repeat
MEL2
Triplicate
MEL3
B
Polydopamine
PDMS/Glass
PDMS / Glass
DTSSP
DTSSP
EKGPGP
EKGPDP
EKGPDP
EKGPDP-modified biosensing surface

Figure 4

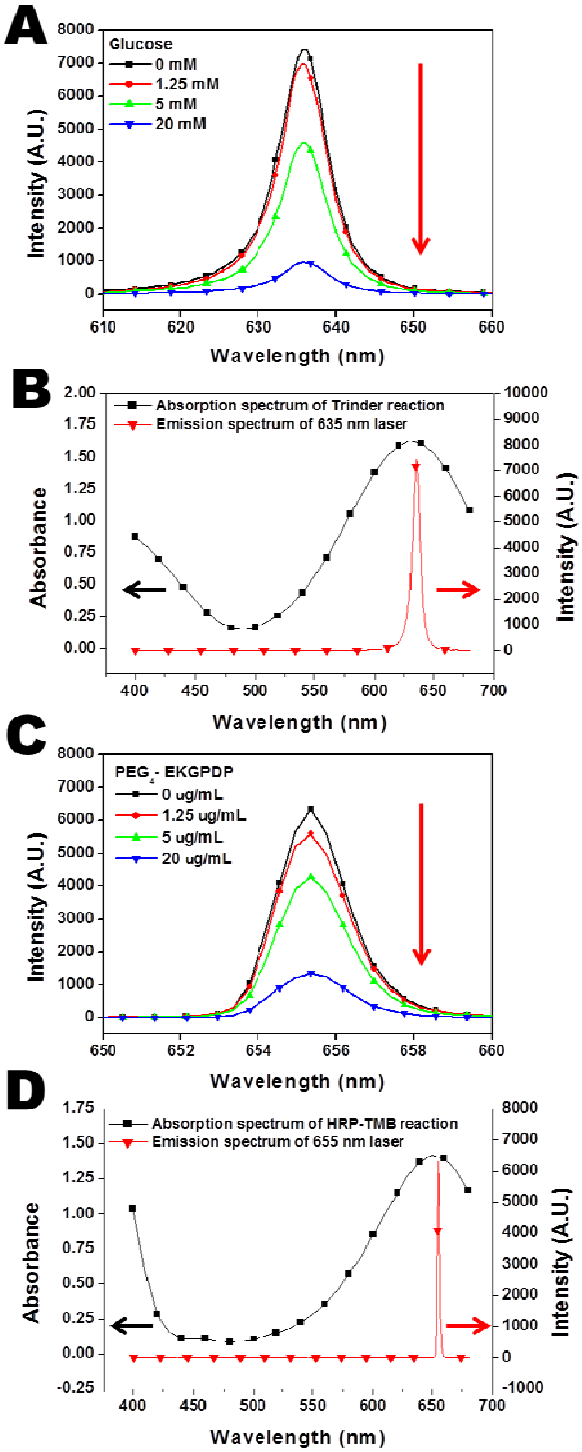

Figure 5

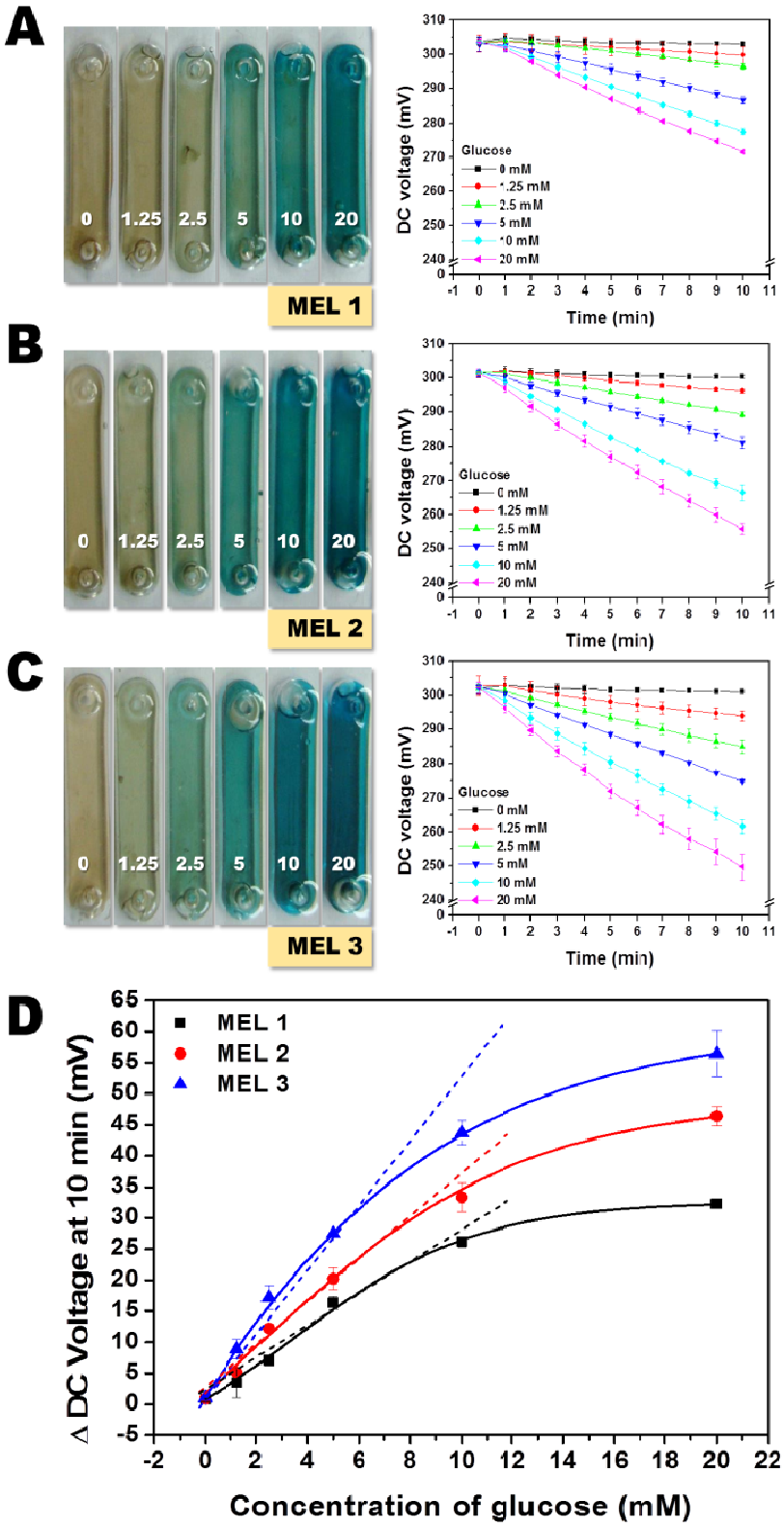

Figure 6

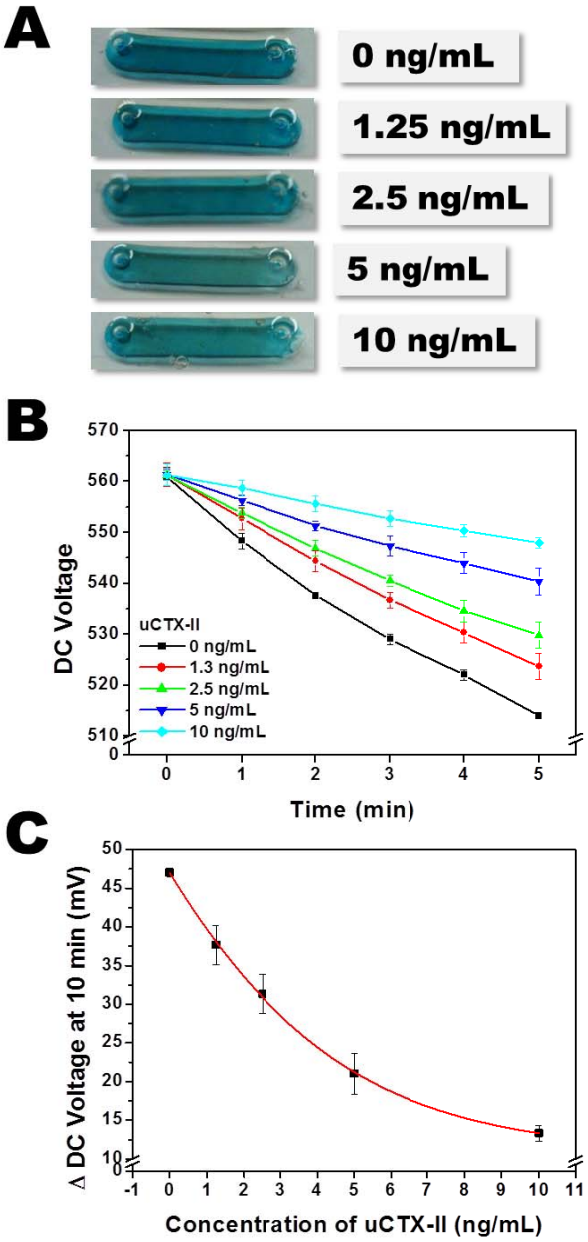

Highlights (BIOS_6665)

- Simple optical transducer was made by assembling common electronics components.
- HRP-mediated colorimetric assay was integrated with the biosensing platform.
- Recognition surfaces were constructed using polydopamine and LBL approach.
- Analyses of an osteoarthritis biomarker and glucose were accomplished.

Graphical abstract: